

Exploring effective factors on energy data of some benzofuran derivatives

Pouya Karimi^{1,*}, Somayeh Makarem² and Hamid Ahmar¹

¹Department of Chemistry, Faculty of Science, University of Zabol, P.O. Box 98615-538, Zabol, Iran

²Department of Chemistry, Karaj Branch, Islamic Azad University of Karaj, Karaj, Iran

Benzofuran derivatives have many useful applications. Computational quantum chemistry method was used to study the relationship between energy data and molecular properties of the 5,6-dihydroxy-2-methyl-1-benzofuran-3-carboxylate derivatives (molecules 3a–3f). Results indicate that there is a good relationship between intramolecular hydrogen bond lengths and energy data of these molecules. Also, X-ray of molecule 3e was used to compare experimental and computational geometrical parameters. Chemical hardness, chemical potential and electronegativity values were calculated to recognize relation between energy data and reactivity of these molecules. Atomic net charges and molecular electrostatic potential values were employed for better insight regarding energy data of the molecules. Electronic charge densities were calculated using atoms in molecules method. The correlation coefficients between experimental and computational ¹³C NMR chemical shifts were examined. Total spin-spin coupling constant and its components were evaluated to understand the contribution of these properties in energy data of the molecules. The relation between energy data of the molecules and aromaticity of the rings was also determined.

Keywords: Benzofuran, computational quantum chemistry, energy data, molecular properties.

BENZOFURAN derivatives show biological activities^{1–3}. Many synthetic benzofuran derivatives are used as antimicrobial^{4–6}, antiviral⁷, antioxidant^{8,9}, antitumour¹⁰, anti-Alzheimer¹¹ and anti-inflammatory¹² agents. Bioactive benzofuran derivatives are found in many essential drugs and products¹³. Moreover, benzofuran and its derivatives have a wide range of biological and pharmacological applications, such as in the treatment of skin cancer¹⁴. Some researchers have studied the medicinal importance of compounds containing benzofuran rings¹⁵.

It has been reported that transformation of skeleton of vitamin E from chroman to benzofuran leads to increase in its antioxidant activity¹⁶. Also, some benzofuran derivatives have shown potential β -amyloid aggregation inhibitory activity¹⁷. The antitumour, antimicrobial, antiviral, anti-inflammatory, anti-hyperglycemic and antipy-

retic activities of benzofuran derivatives have also been discussed in the literature¹⁸.

Syntheses of benzofuran derivatives have been reported in several publications^{19–23}. Also, semi-empirical studies have been performed on benzofuran derivatives. For instance, geometries of the arylalkanoic acids, indomethacin, naproxen and ibuprofen have been optimized using semi-empirical AM1 method and molecular parameters employed for identification of non-steroidal anti-inflammatory agents²⁴.

Synthesis and density functional theory (DFT) studies have been carried out on conformational isomers of the calix[3]benzofurans²⁵. Also, computational thermochemical studies have been performed on benzofuran derivatives and other similar molecules to examine the influence of heteroatoms on the standard enthalpies of formation²⁶. Moreover, some benzofuran derivatives have been studied using molecular docking simulations²⁷. The activity of these molecules against farnesyltransferase has been revealed using structural feature studies²⁸.

We have performed theoretical studies on 5,6-dihydroxy-2-methyl-1-benzofuran-3-carboxylate derivatives (3a–3f) to obtain better insight into the relationship between energy data and molecular properties of these types of molecules. We have also considered correlation between experimental²³ and theoretical ¹³C NMR data to validate the characterization of these molecules. The X-ray spectrum of molecule 3e has been provided to confirm geometrical parameters.

Computational methods

All geometries were optimized at the B3LYP/6-311++G** level of theory with Gaussian 09 program package²⁹. Frequency calculations were performed at the above-mentioned level, and results show that all geometries correspond to true minima with no imaginary frequency. Atomic net charges were calculated utilizing the ChelpG scheme³⁰ at the B3LYP/6-311++ G** level of theory. The topological properties of electronic charge densities were calculated by the atoms in molecules (AIM) method on the wave functions obtained at the B3LYP/6-311++G** level of theory using AIM2000 program³¹. Aromaticity of the six-member rings within each

*For correspondence. (e-mail: pkarimi@uoz.ac.ir)

molecule was calculated using nucleus-independent chemical shift (NICS) and aromatic fluctuation (FLU) indices. Also, multi-centre delocalization (MCDI) criterion was used to calculate aromaticity of the five-member rings. Molecular electrostatic potential (MEP) values were computed to find positions in benzofuran derivatives which are more suitable for hydrogen-bonding interactions.

Results and discussion

Geometrical parameters and energy data

Geometry optimizations of molecules **3a–3f** were performed using Gaussian 09 program package. Scheme 1 shows typical structures of the stable conformations of these molecules and the number of atoms. It should be noted that each of the above-mentioned molecules has a less stable conformation with different dihedral angles $C_5C_4H_{16}H_{17}$ and $H_{19}H_{18}C_5C_4$ compared to stable conformation. Thus, difference between total energies of the two conformations of each molecule (ΔE) was utilized to compare their stabilities. Table 1 shows that order of the ΔE values (kcal mol^{-1}) for the above-mentioned molecules is: **3d** (15.56) < **3a** (15.65) < **3e** (15.89) < **3b** (15.93) < **3f** (16.46) < **3c** (16.56). Geometrical parameters were studied to find relation between these data and ΔE values. Results indicate that there is a relationship between hydrogen bond lengths and ΔE values (■ and ▲ refer to molecules **3a–3c** and **3d–3f** respectively). However, there is no further direct relationship between geometrical parameters and energy data. This implies that intramolecular hydrogen bonding is a key factor which affects energy data of the benzofuran derivatives. Relation between molecular properties such as dipole moments, quadrupole moments, energy gaps and energy data was also studied. As can be seen in Table 1, molecules with larger ΔE values have more

negative values of quadrupole moments. However, there is no meaningful relationship between dipole moments as well as energy gaps and energy data.

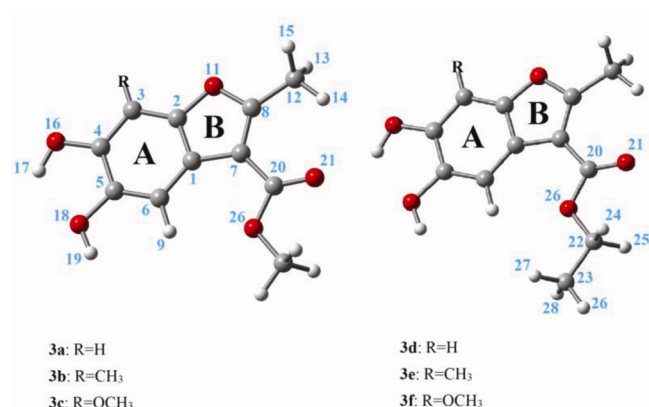
The chemical hardness (η) and chemical potential (μ) were calculated using the highest occupied molecular orbital (HOMO) and lowest unoccupied molecular orbital (LUMO) energies as: $\eta = (I-A)/2$ and $\mu = -(I+A)/2$ where I is the ionization potential and A is the electron affinity of the molecular system.

Electronegativity (χ) is defined as the negative value of chemical potential. Electronegativity and hardness are used to predict chemical reactivity of molecules. The order of electronegativity of molecules **3a–3f** at the B3LYP/6-311++G** level of theory (eV) is: **3e** (3.48) < **3b** (3.50) < **3f** (3.53) < **3c** (3.55) < **3d** (3.57) < **3a** (3.59).

The molecules with large energy gap values are known as hard species and those with small energy gap values as soft species. The order of chemical hardness of these molecules at the above mentioned level (eV) is: **3b** (2.259) < **3e** (2.267) < **3a** (2.274) < **3d** (2.281) < **3c** (2.288) < **3f** (2.295). As can be seen, molecules **3c** and **3f** represent the higher hardness in comparison to other molecules, which implies that these molecules have low chemical reactivity.

The X-ray of molecule **3e** as representative of the above-mentioned molecules was used to compare experimental and computational geometrical parameters. As can be seen in Table 2, there is good correlation between experimental and computational bond lengths and bond angles of these molecules.

Atomic net charges were computed using ChelpG scheme to get better insight into energy data of molecules **3a–3f**. Results indicate that positive atomic charges on C_3 in the molecules with larger ΔE values (**3c** and **3f**) are larger than those for other molecules. Also, sum of atomic charges on rings A and B in the molecules **3c** and **3f** is



Scheme 1. Typical structures of the benzofuran derivatives.

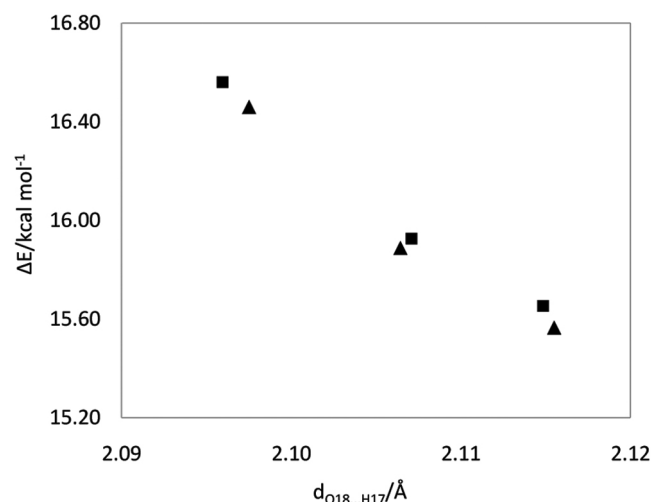


Figure 1. Relationship between hydrogen bond lengths and ΔE values of molecules **3a–3f**.

Table 1. Energy data and electronic properties of 5,6-dihydroxy-2-methyl-1-benzofuran-3-carboxylate derivatives calculated at the B3LYP/6-311++G** level of theory

Molecule	Energy ⁱ	Dipole moment ⁱⁱ	Quadrupole moment ⁱⁱⁱ	HOMO ^{iv}	LUMO ^{iv}	Energy gap ^{iv}
3a	-801.550, <i>-801.525</i>	2.875	-94.061	-5.867	-1.318	4.549
3b	-840.879, <i>-840.854</i>	2.342	-100.337	-5.762	-1.244	4.518
3c	-916.096, <i>-916.070</i>	3.142	-105.527	-5.840	-1.264	4.576
3d	-840.879, <i>-840.855</i>	3.139	-100.522	-5.847	-1.284	4.562
3e	-880.208, <i>-880.183</i>	2.604	-106.801	-5.742	-1.208	4.533
3f	-955.425, <i>-955.399</i>	3.368	-111.883	-5.821	-1.231	4.590

(i)–(iv) are in Hartree, Debye, Debye-Å and eV respectively. Values in italics correspond to less stable conformations.

Table 2. Comparison between experimental (X-ray) and computational geometrical parameters of the stable conformation of molecule **3e** calculated at the B3LYP/6-311++G** level of theory

Bond	Bond length (Å)		Bond	Bond length (Å)	
	Experimental	Computational		Experimental	Computational
C ₂ O ₁₁	1.375	1.379	C ₁ C ₆	1.402	1.401
C ₈ O ₁₁	1.375	1.363	C ₁ C ₂	1.403	1.398
C ₄ O ₁₆	1.37	1.367	C ₁ C ₇	1.444	1.454
C ₂₀ O ₂₆	1.333	1.357	C ₇ C ₂₀	1.458	1.467
O ₂₆ C ₂₂	1.465	1.448	C ₃ C ₄	1.374	1.395
O ₂₁ C ₂₀	1.211	1.214	C ₇ C ₈	1.388	1.373
O ₁₈ C ₅	1.345	1.382	C ₂ C ₃	1.398	1.391
C ₅ C ₆	1.372	1.385	C ₈ C ₁₂	1.448	1.483
C ₄ C ₅	1.433	1.410	C ₂₂ C ₂₃	1.488	1.515

Bond	Bond angle (Å)		Bond	Bond angle (Å)	
	Experimental	Computational		Experimental	Computational
C ₂ O ₁₁ C ₈	106.5	107.5	O ₁₆ C ₄ C ₅	119.3	119.9
C ₂₀ O ₂₆ C ₂₂	117.2	116.1	C ₃ C ₄ C ₅	122.7	121.5
O ₁₈ C ₅ C ₆	123.7	123.8	C ₈ C ₇ C ₁	106.2	106.5
O ₁₈ C ₅ C ₄	114.1	114.0	C ₈ C ₇ C ₂₀	129.1	124.5
C ₆ C ₅ C ₄	122.2	122.2	C ₁ C ₇ C ₂₀	124.7	129.1
C ₆ C ₁ C ₂	118.9	118.6	O ₁₁ C ₂ C ₃	123.2	124.7
C ₆ C ₁ C ₇	135.4	136.1	O ₁₁ C ₂ C ₁	110.7	109.9
C ₂ C ₁ C ₇	105.7	105.3	C ₃ C ₂ C ₁	126.1	125.4
C ₅ C ₆ C ₁	116.9	117.6	C ₄ C ₃ C ₂	113.2	114.6
O ₂₁ C ₂₀ O ₂₆	122.7	122.5	O ₁₁ C ₈ C ₇	110.9	110.8
O ₂₁ C ₂₀ C ₇	123.8	126.0	O ₁₁ C ₈ C ₁₂	114.4	115.7
O ₂₆ C ₂₀ C ₇	113.5	111.6	C ₇ C ₈ C ₁₂	134.7	133.5
O ₁₆ C ₄ C ₃	118.0	118.6	O ₂₆ C ₂₂ C ₂₃	110.8	107.7

Correlation coefficients between experimental and computational values for bond lengths and bond angles are 0.961 and 0.978 respectively.

greater than those for other molecules. Figure 2 reveals that there is a good relation between sum of atomic charges on rings A and B in the molecules **3a–3f** and Hammett constant σ_{meta} of R groups. In fact, electronic properties of R groups effect on distribution of atomic charges on rings A and B and take part in the energy data of these molecules.

NMR calculations

NMR calculations were performed to obtain computational chemical shifts and spin–spin coupling constants in the molecules **3a–3f**. Results presented in Table 3 show that there is good correlation between experimental and

computational ¹³C chemical shift values (correlation coefficients are given in table).

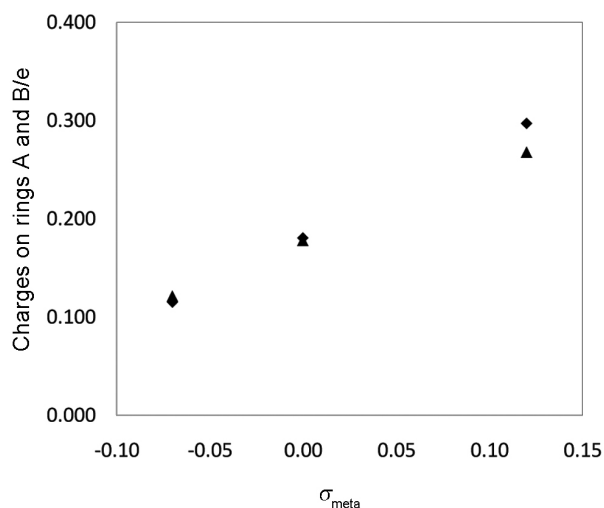
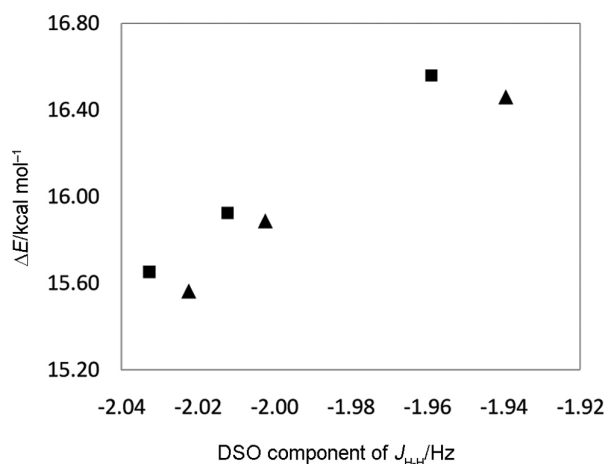
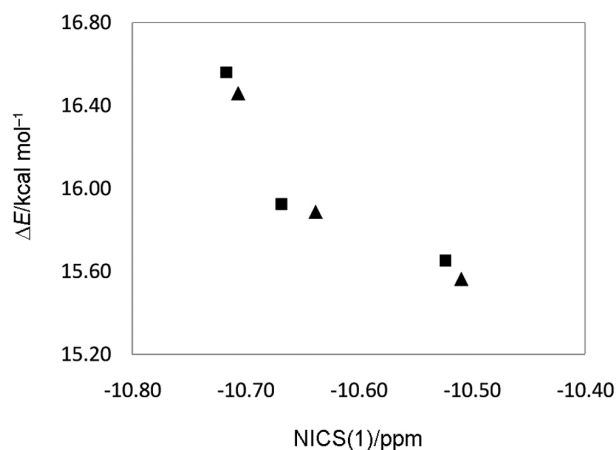
Total spin–spin coupling constant and its components were calculated for the H₁₇–H₁₉ couplings ($J_{\text{H-H}}$) to connect energy data of these molecules to intramolecular couplings. Total spin–spin coupling constant $J_{\text{H-H}}$ has four Fermi-contact (FC), spin-dipole (SD), paramagnetic spin-orbit (PSO) and diamagnetic spin-orbit (DSO) components. Results show that the most important component of $J_{\text{H-H}}$ is DSO in the molecules **3a–3f**. As can be seen in Figure 3, there is a good relation between ΔE values of the molecules and DSO component of $J_{\text{H-H}}$. Thus, diamagnetic spin–orbit contributions of $J_{\text{H-H}}$ take part in

Table 3. Experimental and computational ^{13}C chemical shifts of the stable conformations of 5,6-dihydroxy-2-methyl-1-benzofuran-3-carboxylate derivatives calculated at the B3LYP/6-311++G** level of theory

Experimental	3a	3b	3c	Computational	3a	3b	3c
Me	14.52	14.65	14.62	Me	169.23	169.26	169.25
OMe	51.73	52.46	56.25	OMe	130.29	130.36	130.38
CH of Ar	117.22	116.98	122.12	CH of Ar	80.79	78.05	81.21
C–OH	143.87	143.76	127.25	C–OH	32.82	34.95	39.76
C–OH	144.69	147.18	138.12	C–OH	36.52	36.92	35.72
CO ₂ Me	164.66	165.02	150.12	CO ₂ Me	11.76	11.56	11.68

Experimental	3d	3e	3f	Computational	3d	3e	3f
Me	14.52	14.62	14.62	Me	169.25	169.30	169.28
OEt	14.69, 60.28	14.69, 60.32	14.72, 56.38	OEt	118.72, 168.13	118.82, 168.16	118.75, 168.14
CH of Ar	117.26	116.39	124.51	CH of Ar	80.76	78.04	81.03
C–OH	143.83	142.33	127.20	C–OH	32.91	35.04	39.78
C–OH	144.65	147.13	137.61	C–OH	36.64	37.05	35.80
CO ₂ Me	164.23	164.35	148.78	CO ₂ Me	12.22	11.98	12.10

Correlation coefficients between experimental²³ and computational values for molecules **3a–3f** are 0.993, 0.995, 0.974, 0.949, 0.952 and 0.923 respectively.

**Figure 2.** Sum of atomic charges on rings A and B versus Hammett constants of R groups.**Figure 3.** Correlation between ΔE values of the molecules and DSO component of $J_{\text{H-H}}$.**Figure 4.** Relationship between aromaticity of ring A and ΔE values of molecules **3a–3f**.

stabilization of the benzofuran derivatives. Atoms H₁₇ and H₁₉ correspond to OH groups. Therefore, substitution of benzofuran derivatives with these groups may help increase the stability of the molecules through spin–spin couplings.

The aromaticity of ring A in the molecules **3a–3f** was calculated on the basis of NICS(1) criteria, at 1 Å above the centre of the ring to relate energy data of these molecules to properties of π -electron clouds. Results reveal that the increase in aromaticity of ring A is accompanied by increase of ΔE values (Figure 4). Thus, aromaticity of six-member rings in the benzofuran derivatives is a key factor which contributes to their stability.

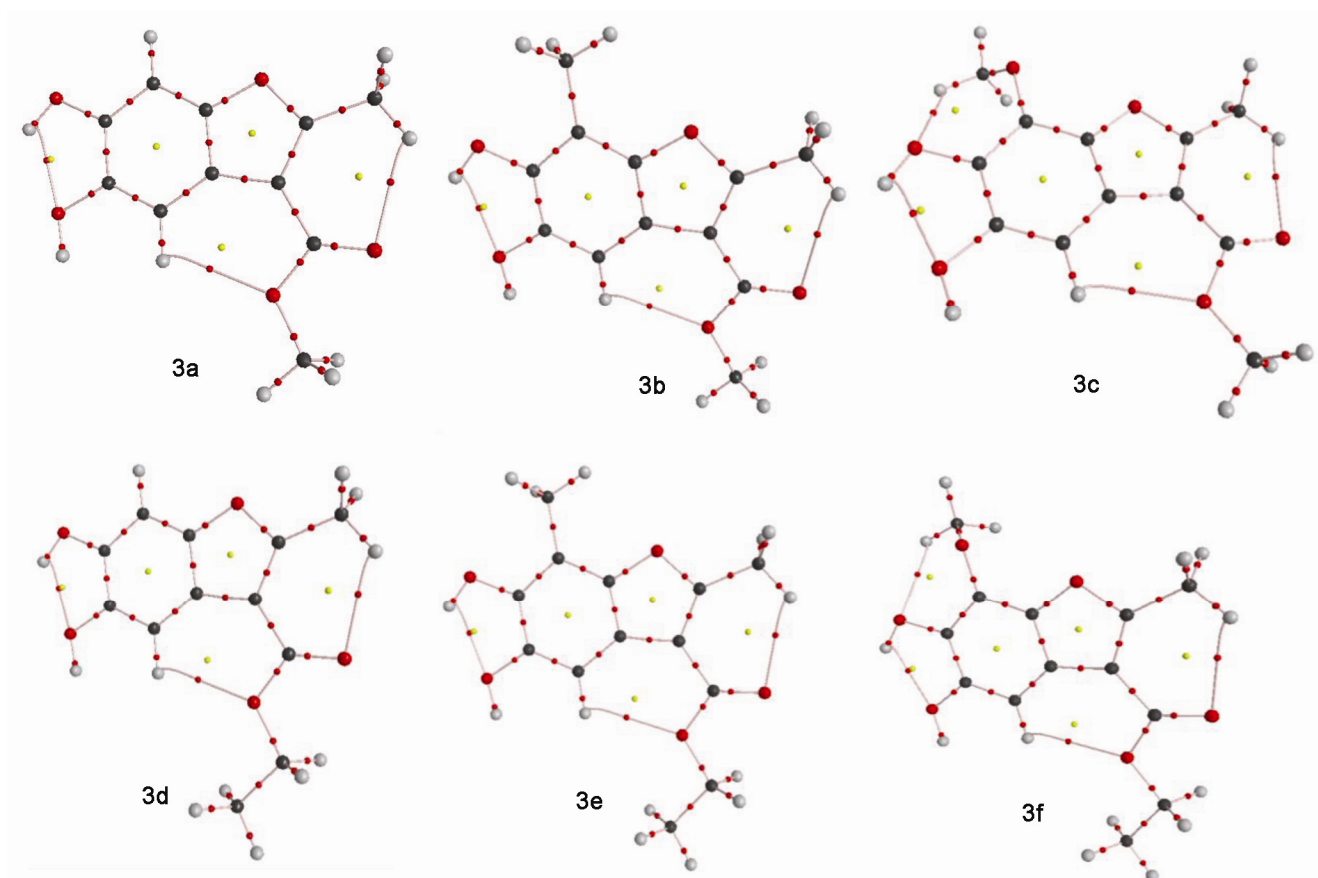
AIM analyses

The topological properties of electronic charge densities were calculated using the AIM method to connect them to

Table 4. Minimum and maximum electrostatic potential (MEP kcal mol⁻¹) and the corresponding coordinates (Å) of stable conformations of benzofuran derivatives calculated at the B3LYP/6-311++G** level of theory

Molecule	MEP	X	Y	Z	X'	Y'	Z'
3a	-32.24	5.33	0.04	0.02	-2.07	-3.98	-0.05
3b	-32.95	5.47	0.71	-0.04	-1.22	-4.42	-0.01
3c	-32.77	5.61	-1.21	0.09	-0.43	4.63	-0.02
3d	-32.89	4.97	1.45	-0.02	-1.26	-4.08	-0.01
3e	-33.60	-4.92	2.13	-0.05	0.40	-4.40	-0.03
3f	-33.39	-4.96	2.50	0.14	-0.24	-4.42	-0.18

X', Y' and Z' refer to coordinates of maximum electrostatic potentials.



Scheme 2. Molecular graphs of benzofuran derivatives showing bond critical points, ring critical points, and bond paths.

energy data of the molecules **3a–3f**. Scheme 2 shows the molecular graphs of these molecules. As can be seen, there are six ring critical points (RCPs) in the molecular graphs of molecules **3c** and **3f** (other molecules have five RCPs). This finding highlights the role of OCH₃ group in the formation of an extra RCP in these molecules. As mentioned, molecules **3c** and **3f** have larger ΔE values in comparison to the other molecules. Therefore, properties of electronic charge densities and number of RCPs seem to play a part in energy data of these molecules. Results indicate that there is a relation between sum of electronic charge density values at RCPs of rings A and B

($\sum \rho_{\text{RCP}(A+B)}$) and ΔE values of the molecules **3a–3f**. In fact, decrease of $\sum \rho_{\text{RCP}(A+B)}$ values is accompanied by increase of ΔE values (Figure 5).

Aromaticity at ring B of the molecules **3a–3f** was calculated using MCDI criterion. Results indicate that the order of MCDI at ring B of these molecules (au) is: **3e** (0.1380×10^2) < **3b** (0.1382×10^2) < **3a** (0.1405×10^2) < **3d** (0.1407×10^2) < **3f** (0.1415×10^2) < **3c** (0.1416×10^2). As can be seen, there is no meaningful relation between aromaticity at rings B and stability of these molecules. On the other hand, aromaticity at ring A was calculated on the basis of FLU benchmark. Results reveal that the

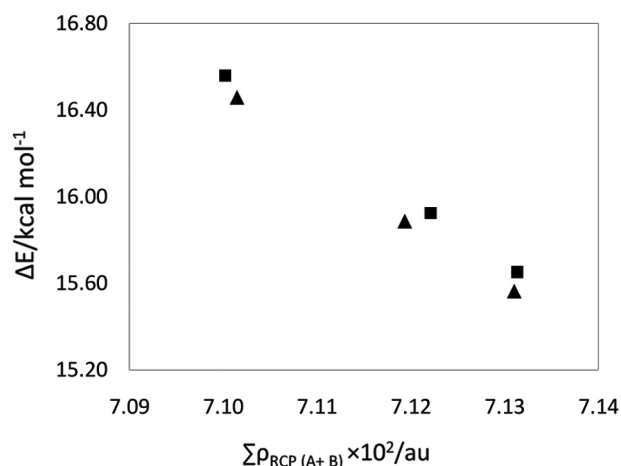


Figure 5. ΔE values of molecules **3a–3f** against electronic charge density values at ring critical points of rings A and B.

order of FLU values at ring A of these molecules is: **3a** \approx **3d** (9.26×10^2) < **3e** (10.36×10^2) < **3b** (10.38×10^2) < **3c** (11.75×10^2) < **3f** (11.76×10^2). As can be seen, FLU values at ring A of molecules **3c** and **3f** are larger than those for other molecules. As mentioned, these molecules have larger ΔE values in comparison to the other molecules. Also, ring A in these molecules on the basis of NICS(1) criterion is more aromatic than the other molecules. Consequently, aromaticity of six-member rings in the benzofuran derivatives is an important factor which contributes to their energy data.

Molecular electrostatic potentials

The most negative MEPs ($V_{s,\min}$) were computed to find positions in benzofuran derivatives which are more suitable for hydrogen-bonding interactions. Table 4 shows all MEPs of molecules **3a–3f**. Coordinates of MEPs in these molecules are also given in the table. Results show that the position of $V_{s,\min}$ is near atom O₂₁ of the above-mentioned molecules. Also, distances between position of $V_{s,\min}$ and atom O₂₁ in molecules with larger ΔE values are shorter than those for other molecules. As can be observed, molecules **3c** and **3f** have the minimum values of $V_{s,\min}$. This finding reveals higher capability of these molecules for hydrogen-bonding interactions through atom O₂₁ in comparison to other molecules. Moreover, results show that the position of the most positive MEPs ($V_{s,\max}$) is close to atom H₁₉ of the molecules **3a–3f**.

Conclusion

Intramolecular hydrogen bonding is a key factor which affects energy data of the benzofuran derivatives. The studied molecules have chemical harnesses in the range 2.259–2.295 eV, which implies that these molecules have

low chemical reactivity. There is a good relation between sum of atomic charges on rings A and B in the molecules **3a–3f** and Hammett constant σ_{meta} of R groups. There is also a good relation between energy data of the molecules and DSO component of $J_{\text{H-H}}$. Aromaticity of six member rings in the benzofuran derivatives is an important factor which contributes to their energy data. MEP results indicate that atoms O₂₁ and H₁₉ of molecules **3a–3f** are the most suitable positions for electrophilic and nucleophilic attack respectively.

Conflict of interest: Authors declare that they have no conflict of interest.

- Lee, S. K., Cui, B., Mehta, R. R., Kinghorn, A. D. and Pezzuto, J. M., Cytostatic mechanism and antitumor potential of novel 1*H*-cyclopenta[*b*]benzofuran lignans isolated from *Aglaia elliptica*. *Chem. Biol. Interact.*, 1998, **115**, 215–228.
- Janprasert, J., Satasook, C., Sukumalanand, P., Champagne, D. E., Isman, M. B. and Wiriyachitra, P., Rocaglamide, a natural benzofuran insecticide from *Aglaia odorata*. *Phytochemistry*, 1992, **32**, 67–69.
- Sundaram, R., Ganesan, R. and Murugesan, G., *In vitro* antiplasmodial activity of spiro benzofuran compound from mangrove plant of southern India. *Asian Pac. J. Trop. Med.*, 2012, **5**, 358–361.
- Jiang, X., Liu, W., Zhang, W., Jiang, F., Gao, Z. and Zhuang, H., Synthesis and antimicrobial evaluation of new benzofuran derivatives. *Eur. J. Med. Chem.*, 2011, **46**, 3526–3530.
- Shankerrao, S., Bodke, Y. D. and Santoshkumar, S., Synthesis and antimicrobial activity of some imidazothiazole derivatives of Benzofuran. *Arab. J. Chem.*, doi:org/10.1016/j.arabjc.2012.10.018.
- Kirilmis, C., Ahmedzade, M., Servi, S., Koca, M., Kizirgil, A. and Kazaz, C., Synthesis and antimicrobial activity of some novel derivatives of benzofuran: Part 2. The synthesis and antimicrobial activity of some novel 1-(1-benzofuran-2-yl)-2-mesitylethanone derivatives. *Eur. J. Med. Chem.*, 2008, **43**, 300–308.
- Malpani, Y. *et al.*, Efficient synthesis of 3*H*,3'*H*-spiro[benzofuran-2,1'-isobenzofuran]-3,3'-dione as novel skeletons specifically for influenza virus type B inhibition. *Eur. J. Med. Chem.*, 2013, **62**, 534–544.
- Rangaswamy, J., Kumar, H. V., Harini, S. T. and Naik, N., Synthesis of benzofuran based 1,3,5-substituted pyrazole derivatives: as a new class of potent antioxidants and antimicrobials-A novel accost to amend biocompatibility. *Bioorg. Med. Chem. Lett.*, 2012, **22**, 4773–4777.
- Rangaswamy, J., Kumar, H. V., Harini, S. T. and Naik, N., Functionalized 3-(benzofuran-2-yl)-5-(4-methoxyphenyl)-4,5-dihydro-1*H*-pyrazole scaffolds: a new class of antimicrobials and antioxidants. *Arab. J. Chem.*, doi:org/10.1016/j.arabjc.2013.10.012.
- Galal, S. A., Abd El-All, A. S., Abdallah, M. M. and El-Diwani, H. I., Synthesis of potent antitumor and antiviral benzofuran derivatives. *Bioorg. Med. Chem. Lett.*, 2009, **19**, 2420–2428.
- Ono, M., Kung, M. P., Hou, C. and Kung, H. F., Benzofuran derivatives as $\text{A}\beta$ -aggregate-specific imaging agents for Alzheimer's disease. *Nucl. Med. Biol.*, 2002, **29**, 633–642.
- Dawood, K. M., Abdel-Gawad, H., Rageb, E. A., Ellithey, M. and Mohamed, H. A., Synthesis, anticonvulsant and anti-inflammatory evaluation of some new benzotriazole and benzofuran-based heterocycles. *Bioorg. Med. Chem.*, 2006, **14**, 3672–3680.
- Radadiya, A. and Shah, A., Bioactive benzofuran derivatives: an insight on lead developments, radioligands and advances of the last decade. *Eur. J. Med. Chem.*, 2015, **97**, 356–376.

14. Hiremathad, A., Patil, M. R., Chand, C. K. R. K., Santos, M. A. and Keri, R. S., Benzofuran: an emerging scaffold for antimicrobial agents. *RSC Adv.*, 2015, **5**, 96809–96828.
15. Nevagi, R. J., Dighe, S. N. and Dighe, S. N., Biological and medicinal significance of benzofuran. *Eur. J. Med. Chem.*, 2015, **97**, 561–581.
16. Masataka, F., Nobuo, M., Tsutomu, H. and Tomihiro, N., Antioxidant activities of vitamin E derivative having benzofuran skeleton. *Nippon Kagakkai Koen Yokoshu*, 2002, **81**, 1381.
17. Rizzo, S., Rivièrè, C., Piazza, L., Bisi, A., Gobbi, S. and Bartolini, M., Benzofuran-based hybrid compounds for the inhibition of cholinesterase activity, beta amyloid aggregation, and abeta neurotoxicity. *J. Med. Chem.*, 2008, **51**, 2883–2886.
18. Shamsuzzaman, H. K., Bioactive benzofuran derivatives: a review. *Eur. J. Med. Chem.*, 2015, **97**, 483–504.
19. Pan, F. and Wiese, G. A., The synthesis and antifungal studies of some benzofuran compounds. *J. Am. Pharm. Assoc.*, 1960, **49**, 259–264.
20. Habermann, J., Ley, S. V. and Smits, R., Three-step synthesis of an array of substituted benzofurans using polymer-supported reagents. *J. Chem. Soc., Perkin Trans.*, 1999, **1**, 2421–2423.
21. Galal, S. A., Abd El-All, A. S., Abdallah, M. M. and El-Diwani, H. I., Synthesis of potent antitumor and antiviral benzofuran derivatives. *Bioorg. Med. Chem. Lett.*, 2009, **19**, 2420–2428.
22. Takahashi, M., Nakano, K. and Nozaki, K., Synthesis and properties of benzophospholo[3,2-*b*]benzofuran derivatives. *J. Org. Chem.*, 2015, **80**, 3790–3797.
23. Fakhari, A. R., Nematollahi, D., Shamsipur, M., Makarem, S., Hosseini Davarani, S. S., Alizadeh, A. and Khavasi, H. R., Electrochemical synthesis of 5,6-dihydroxy-2-methyl-1-benzofuran-3-carboxylate derivatives. *Tetrahedron*, 2007, **63**, 3894–3898.
24. Santana, L. *et al.*, AM1 theoretical study, synthesis and biological evaluation of some benzofuran analogues of anti-inflammatory arylalkanoic acids. *Eur. J. Pharm. Sci.*, 1999, **7**, 161–166.
25. Islam, M. M. *et al.*, Synthesis, structural properties, electrophilic substitution reactions and DFT computational studies of calix[3] benzofurans. *RSC Adv.*, 2016, **6**, 50808–50817.
26. Ramos, F., Flores, H., Rojas, A., Hernández-Pérez, J. M., Camarillo, E. A. and Amador, M. P., Experimental and computational thermochemical study of benzofuran, benzothiophene and indole derivatives. *J. Chem. Thermodyn.*, 2016, **97**, 297–306.
27. Swamy, P. M. G., Prasad, Y. R., Ashvini, H. M., Giles, D., Shashidhar, B. V. and Agasimundin, Y. S., Synthesis, anticancer and molecular docking studies of benzofuran derivatives. *Med. Chem. Res.*, 2015, **24**, 3437–3452.
28. Moorthy, N. S. H. N., Sousa, S. F., Ramos, M. J. and Fernandes, P. A., Structural feature study of benzofuran derivatives as farnesyltransferase inhibitors. *J. Enzyme Inhibit. Med. Chem.*, 2011, **26**, 777–791.
29. Frisch, M. *et al.*, Gaussian 09, Revision A. 1. Gaussian, Inc., Wallingford CT, USA, 2009.
30. Breneman, C. M. and Wiberg, K. B., Determining atom-centered monopoles from molecular electrostatic potentials – the need for high sampling density in formamide conformational analysis. *J. Comput. Chem.*, 1990, **11**, 361–373.
31. Bader, R. F. W., *Atoms in Molecules: A Quantum Theory*, Oxford University Press, Oxford, UK, 1990.

ACKNOWLEDGEMENT. We thank the Vice-Chancellor of Research and Technology at the University of Zabol, Iran.

Received 31 October 2017; revised accepted 17 January 2018

doi: 10.18520/cs/v114/i10/2092-2098